Iranian Journal of Chemical Engineering
Vol. 6, No. 2 (Spring), 2009, IAChE

Research note

Mathematical Modeling of Fluorination Reaction of Uranium Dioxide and Evaluation of Existing Gas-Solid Reaction Models

A. Niksiar, A. Rahimi[*]

Department of Chemical Engineering, College of Engineering, University of Isfahan, Isfahan, Iran.

Abstract

In this study a mathematical model is developed in order to simulate fluorination reaction of uranium dioxide which leads to the production of uranium hexafluoride. The model considers homogeneous reaction for intermediate solid and a heterogeneous one for unreacted shrinking core. Also, this study tries to clearly show the shortcoming of some of the well-known models that take heterogeneous reactions for both solids. In fact, one may not trust the accuracy of those models due to the importance of diffusion phenomena into the intermediate solid and the reaction taking place within it. On the other hand, neglecting the undeniable effects of some operating conditions such as temperature and particle sizes on gas concentration distribution and reaction rates may introduce large deviations. In this study, the governing equations are developed on the basis of the mass conservation law and solved numerically. Besides, for the first time, some dimensionless equations and groups are introduced to predict reaction rates and amounts of the main and intermediate products for use in numerical procedures. Comparing the model results with corresponding experimental ones represents the desirable preciseness of the model. After validation of the model, the effect of some operating variables such as temperature and initial size of the particle are investigated on the reaction rates and conversions.

Keywords: *Fluorination of uranium dioxide, Gas-solid reactions, homogeneous and heterogeneous reactions*

1. Introduction

Gas-solid reactions have wide applications in chemical, petrochemical and metrological industries. These kinds of reactions are classified as heterogeneous and homogenous reactions. If chemical reaction takes place at the solid surface, the reaction is mentioned as heterogeneous. However, the chemical reaction may occur not only at the surface but also on pore walls throughout the solid. The latter is mentioned as homogenous reaction [1]. The choice of an appropriate model is very important due to unpredictable differences between different types of gas-solid reactions. Performing the best selection depends strongly on a correct understanding of the physical and chemical characteristics of the system. In general, the heterogeneous models are more utilized when divided into two simple idealized models: the shrinking particle, and the shrinking unreacted-core models [1].

In a special class of well-known models there are often three steps occurring in succession

∗ Corresponding author: rahimi@eng.ui.ac.ir

during the reaction which involve diffusion of gaseous reactant through the film surrounding the particle, diffusion through the blanket of ash, and reaction of gaseous reactant with the fresh solid. After determining the rate-controlling step by some experimental or analytical treatments, suitable equations may be developed for predicting conversion and temperature variations. The assumptions of some of these models may not precisely match the reality. For example, for a fast reaction situation, the rate of heat release may be high enough, causing significant temperature gradients within the particles or between particle and bulk fluid that may affect the reaction rate. Also, the chemical reaction may occur along a diffuse front rather than along a sharp interface between the ash and fresh solid [2]. Therefore, these models are not realistic for all operating conditions.

On the other hand, gas-solid reactions also have immense applications in uranium conversion processes such as fluorination reaction of uranium dioxide (UO_2) which leads to the production of uranium hexafluoride (UF_6). The overall reaction can be subdivided into two steps. In the first step, a porous solid of uranylfluoride (UO_2F_2) is produced as an intermediate product; and in the second, the intermediate is consumed and the gaseous uranium hexafluoride is produced. The overall reaction is:

$$UO_2 + 3F_2 \rightarrow UF_6 + O_2 \quad (1)$$

in which, it proceeds through the following two steps [3,4]:

$$UO_2(s) + F_2(g) \xrightarrow{k_1} UO_2F_2(s) \quad (2)$$

$$UO_2F_2(s) + 2F_2(g) \xrightarrow{k_2} UF_6(g) + O_2(g) \quad (3)$$

This gas-solid reaction was modeled by Ogata et al. [4, 5]. In their presented model both reactions (2) and (3) were considered as heterogeneous which occur at the surfaces of the unreacted core and the particle itself, respectively. On the basis of this model, the gas F_2 may react at the external surface of the intermediate UO_2F_2 or it diffuses through the bulk of the intermediate, reaches the unreacted core and reacts there. Hence, gas F_2 may diffuse through the solid UO_2F_2 without any reaction, which may not be a realistic assumption. If the ratio of the diffusion rate of F_2 into UO_2F_2 to the reaction rate at the external surface of the particle is low enough, it may be possible to accept this assumption. Whereas in the Ogata and coworkers' study this ratio can be extracted to be as much as 200 [4, 5], leading to the intensification of the theory of homogeneous reaction. Therefore, it appears that this assumption is proposed only in order to implement simple models, and it is not reliable enough to be in conformity with the actual characteristics of the system.

In the previous study of the authors [6], the presented model by Ogata et al. [4, 5] was comprehensively investigated with its whole assumptions. Despite the results presented by Ogata et al. [4,5], considerable deviations were observed between the model results and the experimental data [6]. Let us consider some results presented by Ogata et al. [4, 5] that have been reviewed in the authors' previous study in detail. Fig. 1 shows the time-dependent mole fractions of UO_2, UO_2F_2 and UF_6 which are obtained from this model. The values were compared with the experimental ones reported by Sakurai [7], and as can be seen, are not in appropriate agreement with each other. This result shows the shortcoming of the presented model to predict the reaction rates and conversions correctly.

It should be noted that any other model, presented up-to-now to predict the fluorination process of UO_2 which takes the reactions as heterogeneous ones, contains this shortcoming, basically. Thus, the main aim of this study is to present a useful and precise model to simulate the fluorination reaction of UO_2. For this purpose, a

heterogeneous model is considered for the production reaction of UO_2F_2 and a homogeneous one is considered for its consumption reaction, simultaneously.

2. Mathematical model

Fig. 2 shows the schematic diagram of the model presented in this study.

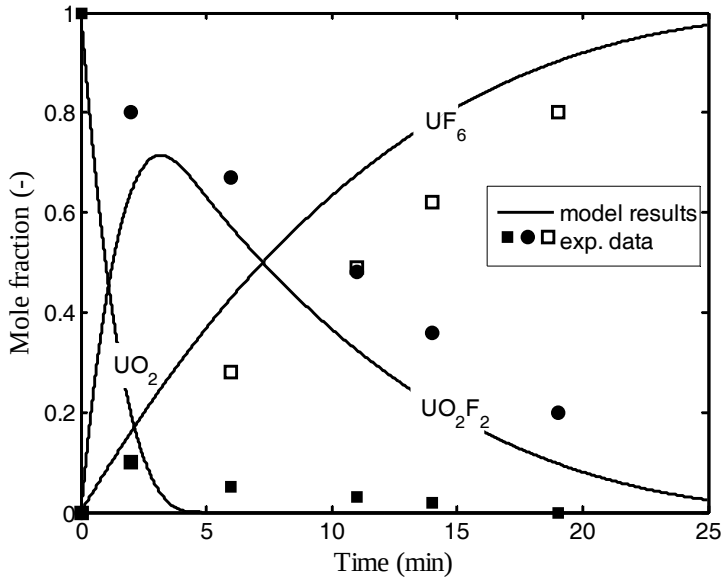

Figure 1. Comparsion of mole fractions of UO_2, UO_2F_2 and UF_6 predicted by heterogeneous reaction model [6] with experimental data reported by Sakurai [7] at T =450°C

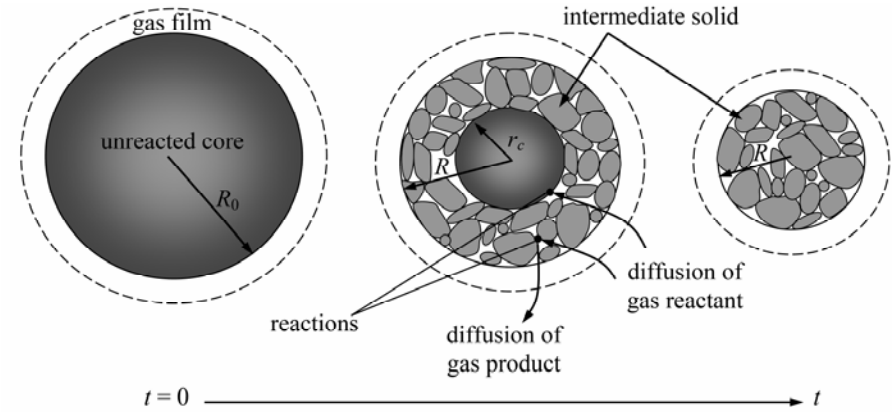

Figure 2. Schematic diagram of a unporous unreacted core with a porous intermediate solid, and the locations of chemical reactions

A mass balance equation for F_2, on a spherical shell of the intermediate solid may give:

$$N_A(4\pi r^2)\Big|_{r+\Delta r} - N_A(4\pi r^2)\Big|_r - r_{A_2}(4\pi r^2\Delta r)a = \varepsilon(4\pi r^2\Delta r)\frac{\partial C_A}{\partial t} \quad (4)$$

where, r_{A_2} is defined as moles of F_2 consumed per unit surface of UO_2F_2 per unit time. a is specific surface area of porous UO_2F_2, and ε is its porosity. By neglecting the convective term of mass transfer, the flux of mass transfer (N_A) is determined as:

$$N_A = D_{eff}\frac{\partial C_A}{\partial r} \quad (5)$$

By substituting Eq. (5) in Eq. (4), and by noting that the reaction (3) is first order with respect to F_2 [8], Eq. (4) is simplified to

$$\frac{1}{r^2}\frac{\partial}{\partial r}(r^2\frac{\partial C_A}{\partial r}) - \frac{k_2 a}{D_{eff}}C_A = \frac{\varepsilon}{D_{eff}}\frac{\partial C_A}{\partial t} \quad (6)$$

Eq. (6) is a partial differential equation that requires an initial condition and two suitable boundary conditions to solve. With a first order reaction (2) with respect to F_2 [5], the boundary conditions are:

$$\text{at } r = r_c \quad : \quad D_{eff}\frac{\partial C_A}{\partial r}\Big|_{r=r_c} = k_1 C_A\Big|_{r=r_c} \quad (7)$$

$$\text{at } r = R \quad : \quad D_{eff}\frac{\partial C_A}{\partial r}\Big|_{r=R} = k_g(C_{Ab} - C_A\Big|_{r=R}) \quad (8)$$

According to the first boundary condition, the diffusion rate of F_2 at the surface of the unreacted core is equal to its reaction rate at the same point. As can be seen, the effect of reaction (2) appears in the boundary conditions due to the heterogeneous nature of this reaction, while reaction (3) occurs in every differential volume within the intermediate solid.

Both boundary conditions are moving due to changes of r_c and R. Therefore, it is necessary to derive appropriate equations in order to determine the instantaneous locations of the boundaries. The required initial condition for Eq. (6) is:

$$at\ t = 0 \quad : \quad C_A = 0 \quad (9)$$

In order to simplify and generalize the solving procedure of Eq. (6) and its boundary conditions, this equation is rewritten in terms of some dimensionless groups, which are defined as follows:

$$\xi = \frac{r}{R_0} \quad ; \quad \tau = \frac{tD_{eff}}{\varepsilon R_0^2} \quad ; \quad C^* = \frac{C_A}{C_{Ab}} \quad (10)$$

where ξ is dimensionless radius, τ is dimensionless time and C^* is dimensionless concentration of F_2. In this situation, Eq. (6) is reduced to:

$$\frac{\partial^2 C^*}{\partial \xi^2} + \frac{2}{\xi}\frac{\partial C^*}{\partial \xi} - \eta C^* = \frac{\partial C^*}{\partial \tau} \quad (11)$$

where, dimensionless parameter η is defined as $\eta = k_2 R_0^2 a / D_{eff}$. As already mentioned, the boundary conditions have specific importance due to their moving nature. The boundary conditions in terms of dimensionless variables are:

$$\text{at } \xi = \xi_C \quad : \quad \frac{\partial C^*}{\partial \xi}\Big|_{\xi=\xi_C} = \frac{R_0 k_1}{D_{eff}}C^*\Big|_{\xi=\xi_C} \quad (12)$$

$$\text{at } \xi = \xi_R \quad : \quad \frac{\partial C^*}{\partial \xi}\Big|_{\xi=\xi_R} = \frac{R_0 k_g}{D_{eff}}(1 - C^*\Big|_{\xi=\xi_R}) \quad (13)$$

k_g is external mass transfer coefficient of F_2, which is determined by the Ranz and Marshall correlation [9]. For a single spherical small particle in a motionless fluid, the Sherwood number is 2. Hence,

$$k_g = \frac{D_{Ag}}{R} \tag{14}$$

where, R is instantaneous radius of the particle. Since, at the surface of the unreacted core the consumption rates of UO_2 and F_2 are equal, the following relation may be written:

$$\frac{dm_{UO_2}}{dt} = \frac{d}{dt}\left[\frac{4}{3}\pi r_c^3 \rho_{UO_2}\right] = (4\pi r_c^2) k_1 C_A\big|_{r=r_c} \tag{15}$$

Therefore,

$$\frac{dr_c}{dt} = \frac{k_1 C_A\big|_{r=r_c}}{\rho_{UO_2}} \tag{16}$$

Eq. (16) may be rewritten in terms of dimensionless variables to give,

$$\frac{d\xi_c}{d\tau} = \frac{\varepsilon C_{Ab}}{\rho_{UO_2}} \frac{k_1 R_0}{D_{eff}} C^*\big|_{\xi=\xi_c} \tag{17}$$

Also, it is necessary to evaluate the variation of particle radius (R) with time. The instantaneous amount of UO_2F_2 is equal to the total amount produced subtracted by the total amount consumed. Also, the total amount of UO_2F_2 produced is equal to the total amount of UO_2 consumed. Thus, the following relation may be written to give the amount of UO_2F_2 at any time:

$$\frac{4}{3}\pi(R^3 - r_c^3)(1-\varepsilon)\rho_{UO_2F_2} = \frac{4}{3}\pi(R_0^3 - r_c^3)\rho_{UO_2} - \sum_{t=0}^{t}\sum_{i(r=r_c)}^{i(r=R)} \frac{1}{2} k_2 C_{Ai} (4\pi r_i^2 \Delta r) a \Delta t \tag{18}$$

The first term on the right hand side of Eq. (18) represents the total produced amount of UO_2F_2, and the second represents the total consumed amount. In fact, the latter shows the total cumulative consumption of UO_2F_2 at any differential volume within the particle. In our numerical technique, this equation is solved by a trial-and-error method to find R, instantaneously. Eq (18) may be rewritten in terms of the dimensionless variables as follows:

$$\xi_R = [\xi_C^3 + \frac{1-\xi_C^3}{1-\varepsilon} - \sum_{t=0}^{t}\sum_{i(r=r_c)}^{i(r=R)} \theta C_i^* \xi_i^2]^{\frac{1}{3}} \tag{19}$$

in which θ is a dimensionless variable which is defined by:

$$\theta = \frac{3}{2}\frac{k_2 a R_0^2}{D_{eff}} \frac{C_{Ab}\varepsilon}{\rho_{UO_2F_2}(1-\varepsilon)} \Delta\tau \tag{20}$$

When Eq. (11) is solved, it is necessary to calculate amounts of the desired materials. Mass of solid UO_2 may be calculated by the following relation:

$$m_{UO_2} = \frac{4}{3}\pi r_c^3 \rho_{UO_2} \tag{21}$$

Corresponding to Eq. (18), mass of solid UO_2F_2 may be calculated by Eq. (22):

$$m_{UO_2F_2} = \frac{4}{3}\pi(R^3 - r_c^3)(1-\varepsilon)\rho_{UO_2F_2} \tag{22}$$

Mass of gas UF_6, which is the desired product, is equal to the amount of UO_2F_2 converted due to reaction (3). Hence:

$$m_{UF_6} = \sum_{t=0}^{t}\sum_{i(r=r_c)}^{i(r=R)} \frac{1}{2} k_2 C_{Ai} (4\pi r_i^2 \Delta r) a \Delta t \tag{23}$$

Furthermore, weight changing of the UO_2 sample, e.g. total instantaneous weight of solids per initial weight of the UO_2 sample, may be calculated by using the expression below:

$$\frac{w}{w_0} = \frac{(4\pi/3)(R^3 - r_c^3)(1-\varepsilon)\rho_{UO_2F_2} + (4\pi/3) r_c^3 \rho_{UO_2}}{(4\pi/3) R_0^3 \rho_{UO_2}} \tag{24}$$

In dimensionless form, Eq. (24) may be simplified to give:

$$\frac{w}{w_0} = \frac{\rho_{UO_2F_2}}{\rho_{UO_2}}(\xi_R^3 - \xi_C^3)(1-\varepsilon) + \xi_C^3 \quad (25)$$

k_1 and k_2 are apparent rate constants of the reactions (2) and (3), respectively, which are calculated by the following equations [4],

$$k_1 = \exp(-\frac{9860}{T} + 5.46) \quad (26)$$

$$k_2 = \exp(-\frac{9450}{T} + 3.59) \quad (27)$$

It should be noted that, since the particle sizes are often very small in the uranium conversion process, the temperature distribution inside the particles is neglected and the model is evaluated at a constant temperature.

3. Numerical solution procedure

Eq. (11) is solved numerically by using the implicit finite difference scheme. As mentioned before, both domain boundaries may move corresponding to the production or consumption of the intermediate solid. In this study, the numerical solution technique which is used is on the basis of the step changing of the domain in order to avoid the use of interpolation methods between general nodal points. In fact, the domain of the intermediate solid is discretised uniformly, and the number and locations of nodal points are not changed until the cumulative consumptions of the solids reach an amount of one $\Delta\xi$. At this moment, due to the production of UO_2F_2 or its consumption, one node is added to or declined from the foregoing number of nodal points. The impreciseness of using this technique reduces strongly when $\Delta\xi$ is taken very small. We divided the whole domain into 101 nodes with dimensionless thicknesses of $\Delta\xi = 0.01$.

In order to do the numerical solution of Eq. (11), it is supposed that a very thin layer of intermediate with dimensionless thickness of 0.02 is presented at the beginning of the process. This assumption is introduced to make use of the initial condition (Eq. 9) easier. The values of temperature, effective diffusivities and the initial radius of the UO_2 particle are presented in Table 1. In addition, the specific surface area of UO_2F_2 is taken to be $a = 4.5\times10^5\ \mathrm{m^2/m^3}$ and its porosity is $\varepsilon = 0.5$ [3].

4. Results and discussion

Fig. 3 shows the model results for the variation of weight changing of the UO_2 sample through the reaction time for $T = 370^\circ\mathrm{C}$ and $T = 430^\circ\mathrm{C}$. The solid reactants consume faster when the temperature is higher. The predicted values are compared with the experimental data reported by Yahata and Iwasaki [3], and they are in a good agreement with each other.

Table 1. Some operating and initial values of required parameters

$T(^\circ C)$	$\mathrm{D_{eff}\,(m^2/s)}$	$R_0\,(m)$	Ref.
450	1.0×10^{-7}	6.7×10^{-6}	[7]
430	1.0×10^{-7}	7.8×10^{-6}	[3]
370	1.0×10^{-7}	7.8×10^{-6}	[3]

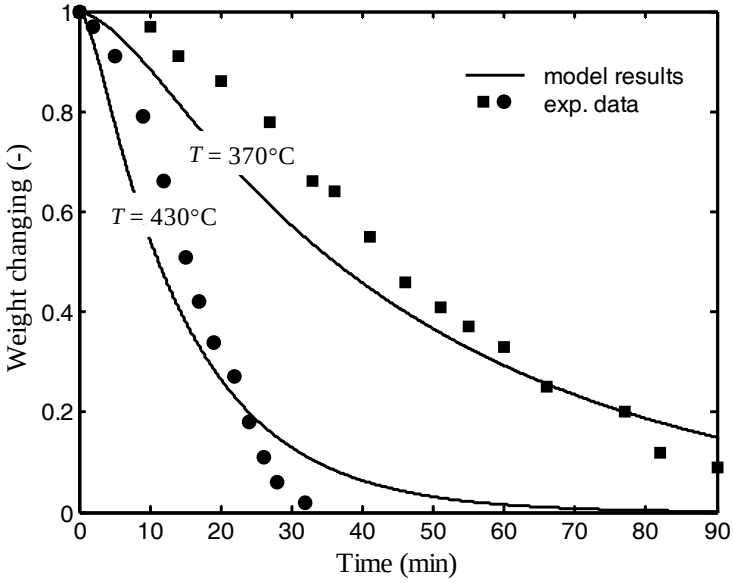

Figure 3. Comparison of predicted weight changing of UO_2 sample with experimental data reported by Yahata & Iwasaki [3]

The time-dependent mole fractions of UO_2, UO_2F_2 and UF_6 are shown in Fig. 4. The values are obtained at $T = 450^{\circ}\mathrm{C}$. The mole fraction of UO_2 decreases quickly and becomes almost zero within 4 min, where the mole fraction of UO_2F_2 reaches about 0.8 of the total moles in a short time. At this time, the amount of UO_2F_2 is high enough to react and produce UF_6. Also, in this figure, the model results are compared with the experimental values reported by Sakurai [7], and as can be seen, they are in good agreement with each other. Thus, by comparing the obtained results in Figs. 1 and 3, one may conclude that the theory of homogenous reaction between UO_2F_2 and F_2 causes more precise results, and the presented model successfully simulates the fluorination reaction of uranium dioxide.

Fig. 5 shows concentration distribution of F_2 within the solid UO_2F_2 and the locations of the unreacted core and the particle fronts as a function of time. The graphs are obtained at $T = 800^{\circ}\mathrm{C}$ and between two limits of $\xi = \xi_C$ and $\xi = \xi_R$. In other words, the width of the graphs shows the thickness of UO_2F_2 at any time. At the beginning of the reactions, the dimensionless radius of the particle is $\xi_R = 1$ and the surface of the unreacted core is very close to the external surface of the particle. In this situation, the concentration distribution of F_2 varies almost linearly with the layer of intermediate. At $T = 800^{\circ}\mathrm{C}$, the ratio of k_1/k_2 is about 4.43. Hence, the diminishing rate of the unreacted-core radius is faster than that for the particle itself. The diffusion resistance increases with the increase of the thickness of the intermediate solid, which causes the decrease of gas concentration at the unreacted core surface. On the other hand, as time passes, the available surface area of the unreacted core, and therefore its reaction rate, decreases. Thus, the forthcoming solid behavior is completely different from that of for the early stages, which is discussed as follows.

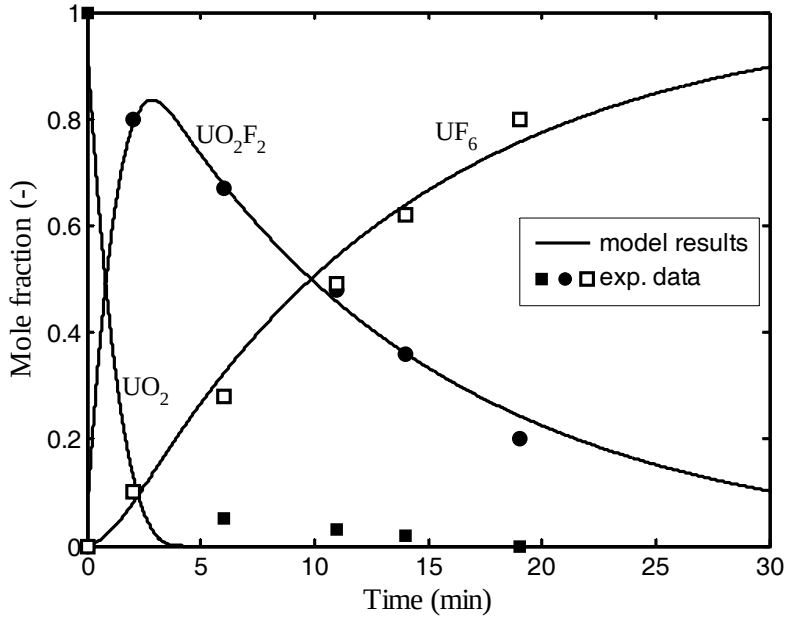

Figure 4. Comparsion of predicted mole fractions of UO_2, UO_2F_2 and UF_6 with experimental data [7] at T=450°C

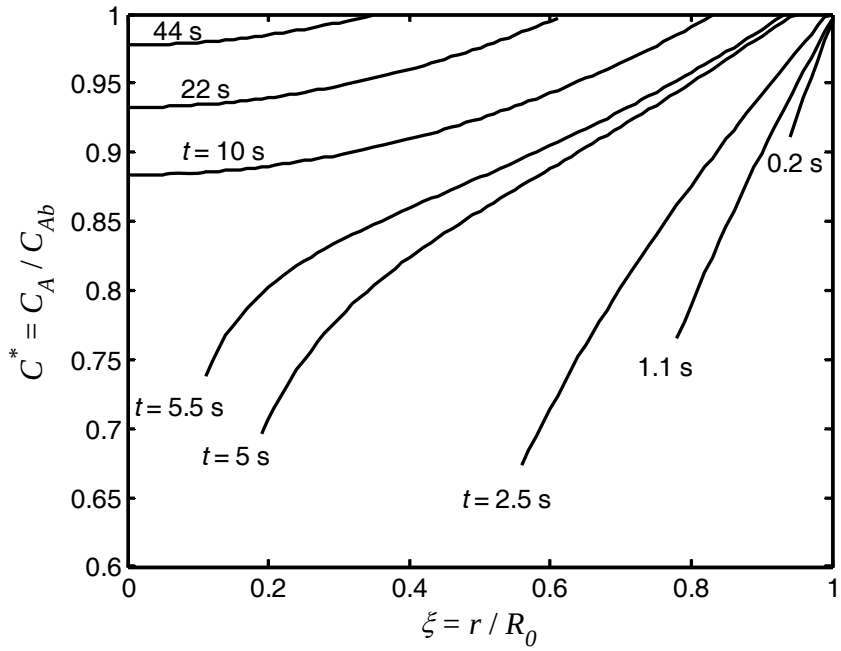

Figure 5. Concentration distribution of F_2 within UO_2F_2 and locations of unreacted core and particle fronts at $T = 800^{\circ}C$

As can be seen in Fig. 5, at large time $(2.5\text{s} < t < 5\text{s})$ although the thickness of the intermediate increases, the gas concentration at the unreacted-core surface increases. This is because of the reduction of the unreacted-core surface, and consequently, the rate of the first reaction. At larger time $(t > 10\text{s})$, in which UO_2 is completely consumed, the dimensionless concentration of F_2 approaches near unity throughout the intermediate domain. The second reaction takes place in all differential volumes of the intermediate as well as at the particle surface. In fact, the diffusion rate of F_2 into UO_2F_2 is high enough that dedicating the second reaction just to the external surface of the particle will impose a large deviation. It should be noted that at lower temperatures the reaction may be the rate-limiting step and the assumption of heterogeneous reaction is wrong.

Another important point that is extracted from Fig. 5 is that, the dimensionless concentration of F_2 is almost unity at the external surface of the particle. This means that the external mass transfer resistance of F_2 is almost negligible at this temperature. It is obvious that at higher temperatures that are more operational, one may easily ignore the resistance of the surrounding gas film.

Fig. 6 shows the radius variations of the particle (R) and the unreacted core (r_c) with time at $T = 450^\circ\text{C}$. The radius of the unreacted core diminishes almost immediately after the reaction begins and reaches zero within 4 min. After this time the only reactant solid is UO_2F_2. According to the correlations (26) and (27), at this temperature the rate constant of reaction (2) is about 4 times greater than that for reaction (3). Hence, a layer of intermediate always exists. Also, Fig. 6 indicates that at the early stages of the reactions, the overall size of the particle remains almost constant while the solids are changing.

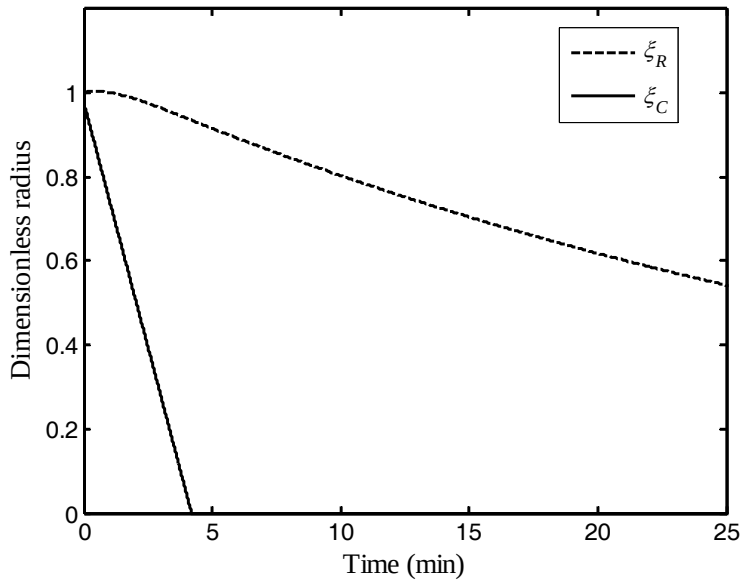

Figure 6. Variation of particle and unreacted core dimensionless radiuses with time at $T = 450^\circ\text{C}$

The reactions rate constants increase with temperature. For temperatures over $1000^{\circ}C$ these constants are about three times higher than that for the temperature range of 370-$450^{\circ}C$ [3]. Therefore, at high temperatures, the reaction rates are significantly higher and consequently, the surface of the unreacted core stays very close to the surface of the particle and the intermediate layer is relatively thin. Fig. 7 represents the locations of the solid surfaces. The abscissa of the figure shows the size of the particle. $1-\xi_C=0$ indicates the initial size of the particle and at $1-\xi_C=1$ the particle completely diminished. The *x*-intercept of the all curves represents the thickness of the intermediate solid when the unreacted core diminishes completely. For example, at $T=2000^{\circ}C$, the unreacted core diminishes when the particle shrinks about 30% of its initial radius. Considering Fig. 7, one can easily investigate the effect of temperature on the whole process.

As mentioned before, at higher temperatures the rates of reactions increase and both reactions take place beside each other. In addition, the external mass transfer coefficient of F_2 increases with temperature, enhancing the reaction rates. As mentioned before, Fig. 7 shows the location of the unreacted core surface relative to the location of the particle surface. As can be seen, the fronts approach each other at higher temperatures.

Fig. 8 illustrates the time-dependent mole fractions of UO_2 and UO_2F_2 for different initial sizes of the particle. In this figure, the solid lines represent the model results for a particle with an initial radius of $R_0=6.5\mu m$ and the broken lines show the same results for a particle with an initial radius of $R_0=20.5\mu m$. As can be seen, both diminishing times of UO_2 and UO_2F_2 increase with the increase of particle initial size. For a larger particle, the necessary time for the unreacted core to diminish will be greater because its diminishing rate decreases due to increasing in the diffusion resistance. In this case, the external surfaces of the solids remain close to each other, which cause the maximum value of UO_2F_2 mole fraction to decrease.

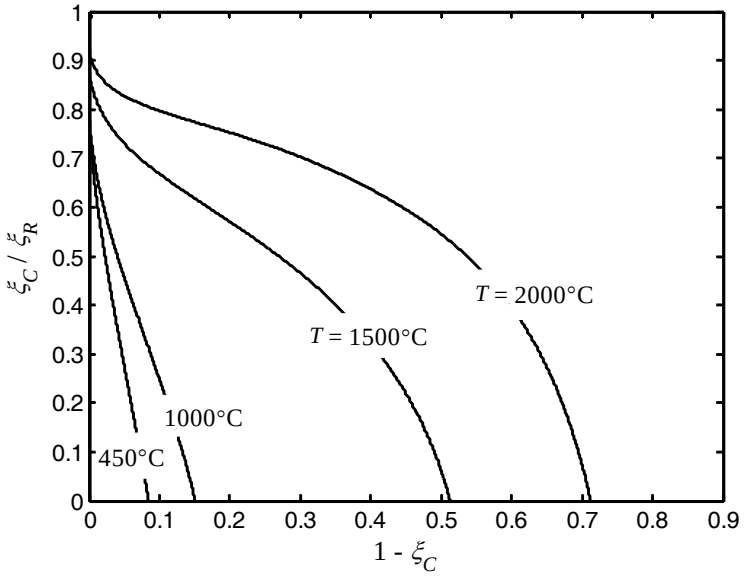

Figure 7. Time-dependent locations of solid surfaces for different operating temperatures

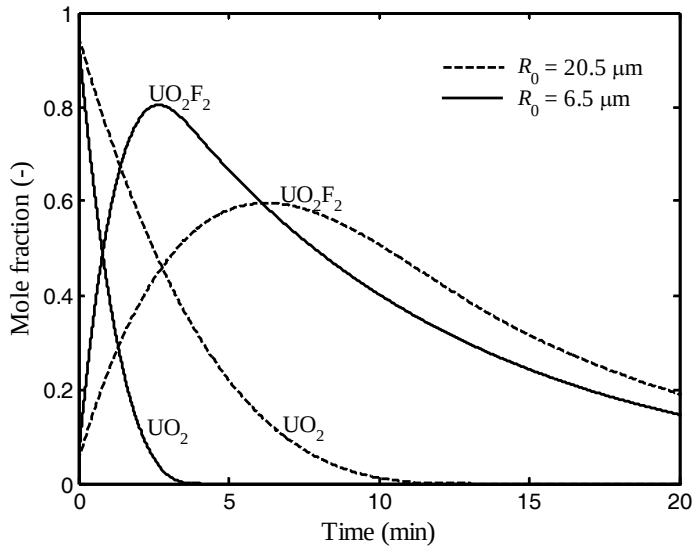

Figure 8. Effect of particle initial size on the time-dependent mole fractions of UO_2 and UO_2F_2

Fig. 9 shows the time-dependent radius of the particle (R) and the unreacted core (r_c) for two different values of the particle initial size. The diminishing rate of the unreacted-core radius decreases sharply with particle initial size, while the diminishing rate of the particle itself remains approximately constant.

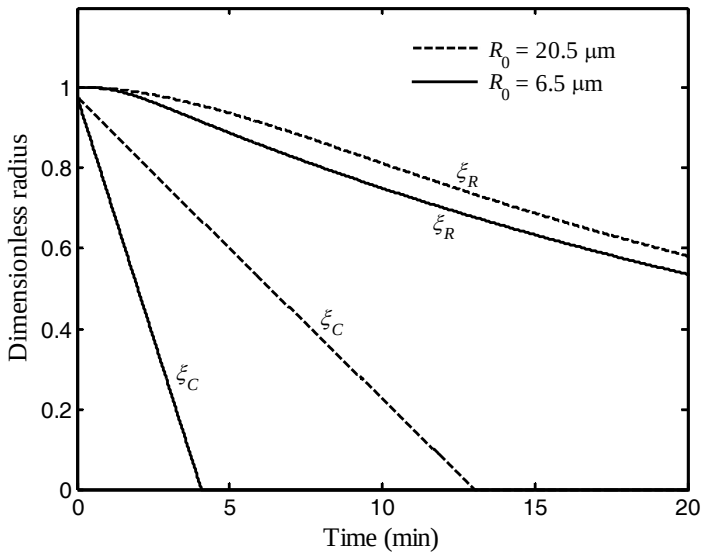

Figure 9. Variation of solid surfaces with time for two different values of particle initial size

5. Conclusion

The mathematical modeling of the fluorination reaction of uranium dioxide is considered by developing a homogenous model for consumption reaction of the solid intermediate and a heterogeneous model for its production reaction. A better agreement is observed between the model results with the experimental data in comparison with the results of the other previously presented models. The results show that at lower temperatures, the chemical reactions are the rate-limiting step. Thus, the consumption reaction of UO_2F_2 occurs along a diffuse front rather than along its external surface. It can be concluded that better understanding of the physical and chemical characteristics of the reactions and material involved, may lead to the selection of a more appropriate model for gas-solid reactions.

Nomenclature

a	specific surface area of UO_2F_2, m^2m^{-3}
C_A	concentration of F_2, $molm^{-3}$
C_{Ab}	bulk concentration of F_2, $molm^{-3}$
C^*	dimensionless concentration of F_2
D_{eff}	effective diffusivity of F_2 into the solid, m^2s^{-1}
D_{Ag}	diffusivity of F_2 into the gas film, m^2s^{-1}
k_1	rate constant for reaction (2), ms^{-1}
k_2	rate constant for reaction (3), ms^{-1}
k_g	mass transfer coefficient, ms^{-1}
m_{UO_2}	mass of UO_2, mol
$m_{UO_2F_2}$	mass of UO_2F_2, mol
m_{UF_6}	mass of UF_6, mol
N_A	mass transfer flux, mol $m^{-2}s^{-1}$
r_c	radius of unreacted core, m
R	radius of particle, m
R_0	initial radius of particle, m
t	time, s
w	weight of solids, mol
w_0	initial weight of solid sample, mol

Greek symbols

ξ	dimensionless radius
ξ_C	dimensionless radius of unreacted core
ξ_R	dimensionless radius of particle
ρ_{UO_2}	density of UO_2, $molm^{-3}$
$\rho_{UO_2F_2}$	density of UO_2F_2, $molm^{-3}$
ε	porosity of UO_2F_2
τ	dimensionless time

References

1. Cussler, E. L., Diffusion mass transfer in fluid systems. Cambridge University Press, (2003).
2. Levenspiel, O., Chemical reaction engineering. 3rd Ed, John Wiley $ Sons, New York, (2001).
3. Yahata, T., Iwasaki, M., "Kinetic studies of the fluorination of uranium oxides by fluorine-part II". Journal of Inorganic Nuclear Chemistry, 26, 1863-1867, (1964).
4. Ogata, S., Homma, S., Sasahira, A., Kawamura, F., Koga, J., Matsumoto, S., "Fluorination reaction of uranium dioxide by fluorine". Journal of Nuclear Science and Technology, 41, 135-141, (2004).
5. Ogata, S., Homma, S., Koga, J., Matsumoto, S., "Gas-solid reaction model for a shrinking spherical with unreacted shrinking core". Chemical Engineering Science, 60, 4971-4980, (2005).
6. Niksiar, A., Rahimi, A., "The evaluation of unreacted shrinking core model for modeling and simulation of fluorination of uranium dioxide". The First International Congress of the Rule of Nuclear Cycle in Research Development and Technology, Isfahan, Iran, (2006).
7. Sakurai, T., "Comparison of the fluorination of uranium dioxide by bromine trifluoride and elemental fluorine". Journal of Physical Chemistry, 78, 1140-1144, (1974).
8. Iwasaki, M., "Kinetics of the fluorination of uranium dioxide pellets by fluorine". J. Nucl. Mater., 25, 216, (1968).
9. Ranz, W.E., Marshall, W.R., "Evaporation from drops". Chemical Engineering Progress, 48, 173-180, (1952).